FUDMA Journal of Sciences (FJS)
ISSN online: 2616-1370
ISSN print: 2645 - 2944
Vol. 8 No. 3, June, (Special Issue) 2024, pp 319 - 330
DOI: https://doi.org/10.33003/fjs-2024-0803-2552

GEOCHEMISTRY AND GENETIC IMPLICATIONS OF BASEMENT ROCKS AROUND MAKARFI AREA, NORTHWESTERN NIGERIA BASEMENT COMPLEX

Raliya Aminu Hayatu

Department of Geology Bayero University, Kano

*Corresponding authors' email: raminuhayatu@gmail.com

ABSTRACT

Major and trace element analysis of rocks around Makarfi were carried out using Inductively Coupled Plasma Mass Spectrometry (ICP-MS) to determine the geochemical characteristics of the lithological components of the area. The area is composed of migmatite gneiss, biotite gneiss, granite gneiss, schists and granites. Analysis for major, trace and REE revealed that the gneisses, are paragneisses and metaluminous. The granites are peraluminous (A/CNK>1) and calc-alkaline. The granites had undergone changes from a more primitive hornblende-biotite I-type variety to a more fractionated muscovite bearing S-type variety. Chemical data shows that the peraluminosity and enrichment in Li, Rb, Cs, Ta, Sn, Nb and Ga increases in the course of differentiation and evolution from hornblende-biotite granite to muscovite granite. Signatures of biotite and muscovite granites suggest emplacement in a syn-collisional tectonic setting while those of hornblende-biotite granite suggest a post-collisional tectonic setting.

Keywords: Peraluminous, Metaluminous, Calc-alkaline, Paragneisses, Syn-collisional, Post-collisional

INTRODUCTION

The Nigerian Basement lies within the reactivated part of the Pan-African belt which is believed to have evolved as a result of collision (collision type orogeny) between the passive continental margin of the West African craton and the active continental margin of the Tuareg shield about 600 Ma ago (Burke and Dewey 1972; Black et al 1979; Ajibade et al 1987). The sequence of events and rock types recognized in some parts of Nigeria can be correlated with similar sequences in Ghana, Togo and Dahomey and Ahaggar, and the sequence of events in the Ahaggar demonstrate quite convincingly the true orogenic nature of the Pan-African in the Ahaggar (McCurry 1976). Thus, the evolution of the Nigerian basement can be best discussed in the regional context of the Pan-African belt of West Africa (Ajibade et al 1987). According to McCurry (1976), the Pan-African orogeny in these areas was the result of the opening and closing of a small sea comparable in size to the red sea. Closure of the ocean at the cratonic margin and crustal thickening (the collision at the cratonic margin led to the reactivation of the Dahomeyen to form a Tibetian-type crust led to the metamorphism and deformation of sediments, partial melting of the thickened crust (upper mantle and lower crust) and the generation of granitic magmas that resulted in the emplacement of the Pan-African granites in Nigeria (Ajibade et al 1987). Ajibade et al (1987) based on a number of geochemical and isotopic data available on the Pan-African granites concluded that the Granitoids are calc-alkaline to alkaline, and that the magmas were derived from mantle sources but were heavily contaminated by crustal materials and also by partial melting of the lower crust. On the other hand, Rahaman (1988) suggested the coexistence of several magmas within the Nigerian Pan-African granites.

Regional Geology

Nigeria is underlain by Precambrian basement complex rocks, Younger Granites of Jurassic age and Cretaceous to Recent sediments (Fig. 1). The Precambrian geology of Nigeria consists of three broad lithological groups; the migmatite gneiss complex, (is polycyclic in nature and widespread throughout the country); the metasedimentary and metavolcanic rocks which form the schist belts (upper Proterozoic); and the older granites which intruded both the migmatite gneiss complex and the schist belts (Pan-African).

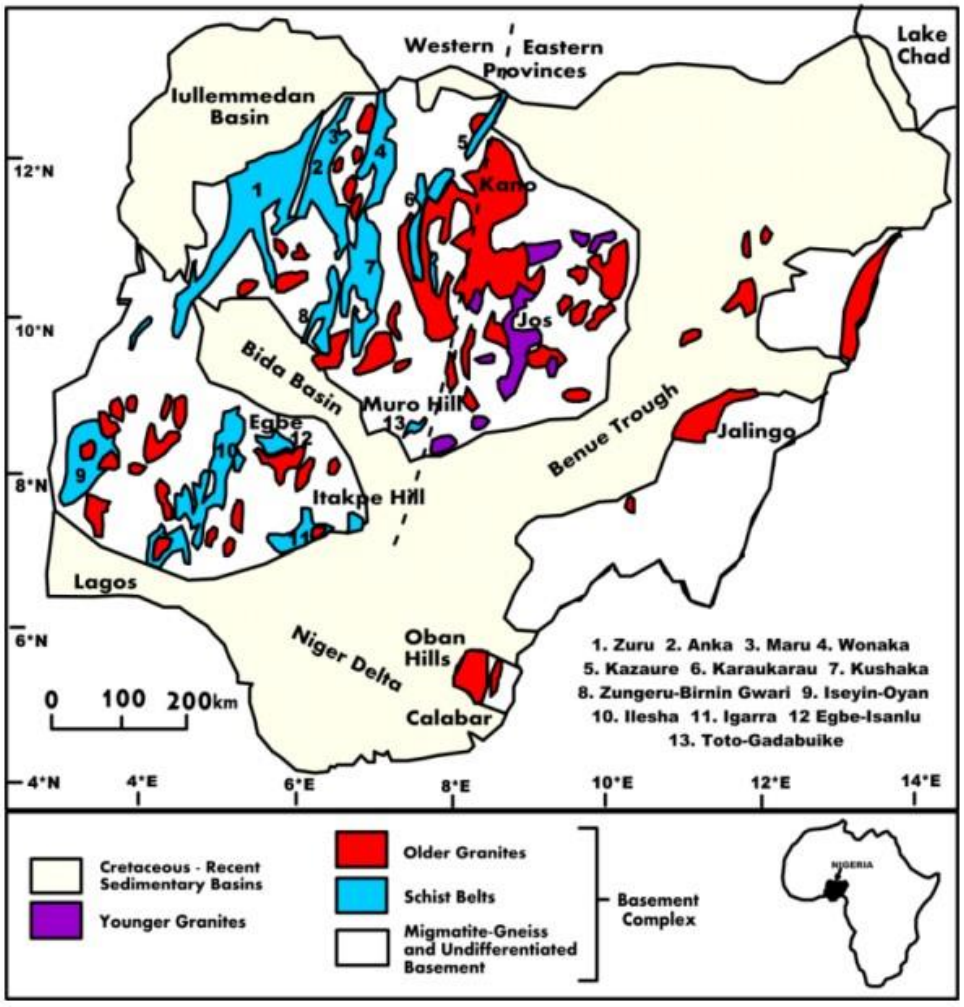

Figure 1: Geological map of Nigeria (adopted from Ogunyele 2018).

The review and description of the Basement Complex of Nigeria has been carried out by several workers and two distinct provinces (Western and eastern provinces) have been recognized in the Nigerian basement complex. The western province is characterized by narrow grade schist belts, and each belt is separated from the others by migmatites and gneisses or granites; while the eastern province comprises mostly of migmatites, gneisses, large volumes of Pan-African granites and Mesozoic granites (Ajibade et al 1976). Evolution of the Nigerian basement is believed to be best understood in the western region, particularly the Northwest which is the most interesting area of basement geology in the north because all the major rock units are present thus enabling a more comprehensive and clearer picture of the basement evolution to be developed (McCurry 1976). Hence this study seeks to investigate the geochemical characteristics of some basement rocks around Makarfi area, Northwestern Nigeria, with a view to understanding their generation and emplacement within the framework of the Pan-African. The area is underlain by gneisses, schist and granites as major rocks, together with pegmatites, mylonite and aplites as minor lithologies (Fig. 2). Detailed field geology and petrography of rocks in the study area are described elsewhere (Hayatu and Ibrahim 2024).

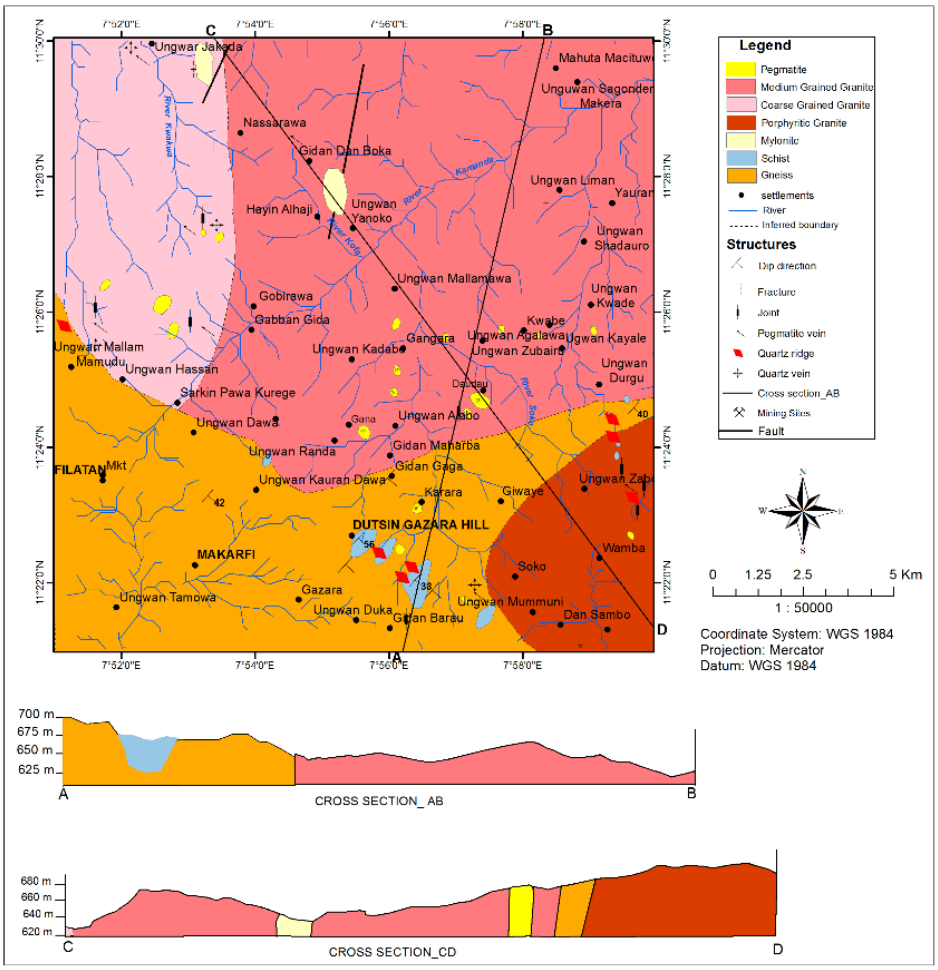

Figure 2: Geological map of the study area

MATERIALS AND METHODS

Analytical Methods

Geochemical analysis of collected rock samples was carried out at the Activation laboratories Ontario, Canada using a lithium metaborate/tetraborate fusion ICP-MS technique for major, minor and trace elements (including REE). The samples analysed comprised three (3) gneisses, three (3) granites and one (1) mylonite. Various discrimination plots were used to classify the granites, determine their tectonic setting, infer their evolution and petrogenesis.

RESULTS AND DISCUSSION

Geochemistry of the rocks

Whole rock geochemical analysis data (Tables 1,2 and 3) provided information on the elemental concentration of the host rocks which provided the basis for a comprehensive rock classification, identification of the original tectonic setting, determination of the fractionation trends, study the inter relationship between elements in order to infer geochemical processes and to deduce the origin and evolution of rocks, as well as petrogenesis. The major element composition of the host rocks plotted on Harker diagram using SiO_2 as an index of differentiation (Figure 3a and b) show that TiO_2, Al_2O_3, Fe_2O_3, MgO, CaO and P_2O_5 are all negatively correlated with SiO_2, while Na_2O and K_2O are positively correlated. From the geochemical data plotted on the classification diagram total alkali silica versus silica (TAS) of Cox *et al*., (1979) (Figure 4a), all the granites plot within the granite field. On the Debon La Forte B-A (1983) plot, the granites plot in different fields revealing their mineralogical compositions (Figure 4b). The biotite and muscovite granites plot within the highly fractionated calc-alkaline field while the hornblende-biotite granite plots within the calc-alkaline and strongly peraluminous field on the discrimination diagram of Sylvester (1989) (Figure 5a). The granites are strongly peraluminous with aluminium saturated index (ASI) ranging from (1.01 to 1.20) and modified alkali- lime index (MALI) ranging from 4.48 to 8.30 (see table S1 in supplementary data). Similarly, all the granites are peraluminous in character as shown on the ANK versus A/CNK discrimination diagram after Shand (1943) (Figure 5b). Molecular A/CNK versus SiO_2 after Chappel and White (1974) was used to classify the rocks into their magmatic origin. On this diagram, the granites occupy both the I-type and S-type granite fields (Figure 6a). Furthermore, the mylonite and gneisses have sedimentary protolith except granite gneiss which plots within the igneous protoliths field as shown on the TiO_2 versus SiO_2 discrimination diagram after Tarney, (1976) (Figure 6b). A spider diagram for the granites normalized to chondrites (Thompson 1982) (Figure 7a) shows that all the granites have pronounced negative K and Ti with weak Ba, Sr and P negative anomalies. They also have a slight positive Rb, Th, Nb and Ta anomalies. The spider diagram of the gneisses (Figure 7b) shows similar pattern. On the R1-R2 tectonic discrimination diagram of Batchelor and Bowden (1985) (Figure 8), all the granites plot within the syn-collisional field. On the Rb versus Y+Nb plot and the Rb versus Ta+Yb plots of Pearce *et al*., (1984) the biotite and muscovite granites plot

largely within the syn-collisional granite field while the hornblende-biotite granite plots within the volcanic-arc granite field. (Figure 9). Furthermore, on the Hf-Rb/30-Ta*3 ternary plots of Harris *et al*., (1986) (Figure 10), the biotite and muscovite granites plot within the syn-collisional granite field, while the porphyritic granite plots within the late to post-collisional granite field. The REE pattern of the granites (Figure 11a) display enrichment of the light rare earth elements (LREE) and depletion in the heavy rare earth elements (HREE). The degree of fractionation of the LREE relative to HREE (LaN/YbN) is moderate with values ranging from (5.85 to 24.8). They also display a negative Eu anomaly as seen from the REE pattern and Eu/Eu* (<1). The REE pattern of the gneisses (Figure 11b) display enrichment in LREE and slight deflection in HREE. The degree of fractionation of the LREE relative to HREE (LaN/YbN) is low with values ranging from (3.42 to 5.13). The gneiss has a negative Eu anomaly except migmatite gneiss which display a very weak positive Eu anomaly and Eu/Eu* of (1.27). Mylonite has a positive Ce anomaly with a weak negative Er anomaly, and the degree of fractionation of the LREE relative to HREE (LaN/YbN) is equally low.

Table 1: Major element data of rocks in the study area (wt %)

Sample/type	**Gneisses**			**Mylonite**		**Granites**	
Oxides	**R_2**	**R_3**	**R_7**	**R_1**	**R_4**	**R_5**	**R_6**
SiO_2	73.09	50.13	54.9	78.38	73.85	73.33	68.93
Al_2O_3	12.65	14.91	16.77	11.94	14.16	13.85	14.63
$Fe_2O_{3(T)}$	2.81	11.28	9.04	2.04	1.66	1.65	3.02
MnO	0.053	0.235	0.128	0.087	0.024	0.037	0.048
MgO	0.14	4.25	1.98	0.44	0.22	0.11	0.91
CaO	0.76	13.32	12.06	0.01	0.95	0.2	2.68
Na_2O	4.27	0.81	1.9	0.15	4.13	3.61	3.59
K_2O	4.43	0.69	0.32	3.79	4.5	4.89	3.57
TiO_2	0.181	1.851	1.165	0.231	0.113	0.103	0.405
P_2O_5	0.03	0.27	0.13	<0.01	0.09	0.07	0.14
LOI	0.36	0.75	1.43	2.08	0.86	0.97	0.68
Total	98.76	98.51	99.83	99.15	100.6	98.83	98.6
A/CNK	0.96	0.57	0.66	2.73	1.06	1.19	0.99

Table 2: Trace elements composition of the rocks in the study area (ppm)

Sample/type	**Gneisses**			**Mylonite**		**Granites**	
Elements	**R2**	**R3**	**R7**	**R1**	**R4**	**R5**	**R6**
Sc	4	33	23	36	3	1	4
Be	5	3	<1	15	7	12	3
V	<5	247	301	9	12	5	42
Ba	362	366	212	42	633	180	915
Sr	59	178	186	3	150	44	598
Y	82	46	16	1	13	26	12
Zr	304	234	88	5	72	77	173
Cr	<20	100	80	<20	<20	<20	20
Co	53	77	68	127	80	66	75
Ni	<20	70	30	<20	<20	<20	<20
Cu	<10	<10	<10	<10	20	20	<10
Zn	50	110	60	50	30	<30	80
Ga	27	21	40	103	23	23	22
Ge	2	2	6	3	1	2	1
As	<5	<5	<5	<5	<5	<5	<5
Rb	132	10	13	994	202	356	131
Nb	25	18	4	115	7	17	10
Mo	<2	<2	<2	<2	<2	<2	<2
Ag	1	0.7	<0.5	<0.5	<0.5	<0.5	0.6
In	<0.2	<0.2	<0.2	0.5	<0.2	<0.2	<0.2
Sn	4	3	<01	306	6	6	2
Sb	<0.5	<0.5	0.6	<0.5	<0.5	<0.5	0.9
Cs	0.8	1.2	3	149	11.5	14.8	10.1
Hf	8.7	5.7	2.2	0.4	2.3	2.5	4.4
Ta	2	1.6	0.7	25.1	1.5	4.8	1.6
W	382	304	336	849	558	479	509
Ti	0.6	<0.1	0.1	2.4	0.9	1.7	0.8
Pb	11	7	7	13	54	41	23
Bi	<0.4	2.7	0.4	41.7	<0.4	<0.4	<0.4
Th	21	4.9	1.6	0.4	7.9	18.3	10.3
U	3.1	0.9	0.6	0.2	32	20.6	2.2

Ratios							
K/Rb	278.59	572.79	204.34	31.65	184.92	114.02	226.23
K/Cs	45968.4	4723.24	885.47	211.15	3248.33	2742.79	2934.22
K/Ba	101.59	15.65	12.53	749.09	59.01	225.52	32.39
Rb/Cs	165	8.33	4.33	6.67	17.56	24.05	12.97
Rb/Sr	2.24	0.06	0.07	331.33	1.35	8.09	0.22
Al/Ga	0.248	0.376	0.222	0.061	0.326	0.319	0.352
Th/U	6.77	5.44	2.67	2	0.25	0.89	4.68
Zr/Hf	34.94	41.05	40	12.5	31.3	30.8	39.32
Zr/Y	3.7	5.09	5.5	5	5.54	2.96	14.42

Table 3: Rare earth elements composition of the rocks in the study area (ppm)

	Gneisses			**Mylonite**		**Granites**	
Elements	**R_2**	**R_3**	**R_7**	**R_1**	**R_4**	**R_5**	**R_6**
La	77	24.6	10.6	1.5	10.9	22.8	33.5
Ce	160	53.2	19.4	15.5	20.2	54.5	68.1
Pr	17.9	6.93	2.4	0.31	2.32	5.66	7.57
Nd	64.4	29	9.7	1.1	8.4	20.2	27.8
Sm	13.9	7.3	2.5	0.2	2	4.8	5.1
Eu	1.25	2.03	1.11	<0.05	0.45	0.38	1.26
Gd	13.1	8.2	2.9	0.2	2	4.6	3.8
Tb	2.3	1.4	0.5	<0.1	0.3	0.8	0.5
Dy	15.4	8.9	3.2	0.2	1.9	4.9	2.4
Ho	3.2	1.7	0.6	<0.1	0.3	0.9	0.4
Er	9.5	4.9	1.8	0.1	0.9	2.5	1.1
Tm	1.47	0.71	0.25	<0.05	0.12	0.39	0.15
Yb	10	4.8	1.8	0.2	0.8	2.6	0.9
Lu	1.49	0.71	0.28	0.04	0.12	0.4	0.13
Sum	390.91	154.38	57.04	19.35	50.71	125.43	152.71
	Normalized ratios						
Eu/Eu*	0.28	0.81	1.27	NA	0.69	0.25	0.88
LaN/YbN	5.13	3.42	3.93	5.00	9.08	5.85	24.81
LaN/SmN	3.41	2.07	2.61	4.61	3.35	2.92	4.04
EuN/YbN	0.36	1.21	1.76	NA	1.61	0.42	4.00

Legend;
R2= Granite gneiss.
R3=Biotite gneiss
R7=Migmatite gneiss
R1= Mylonite
R4=Biotite granite
R5=Muscovite granite
R6=Hornblende-biotite granite

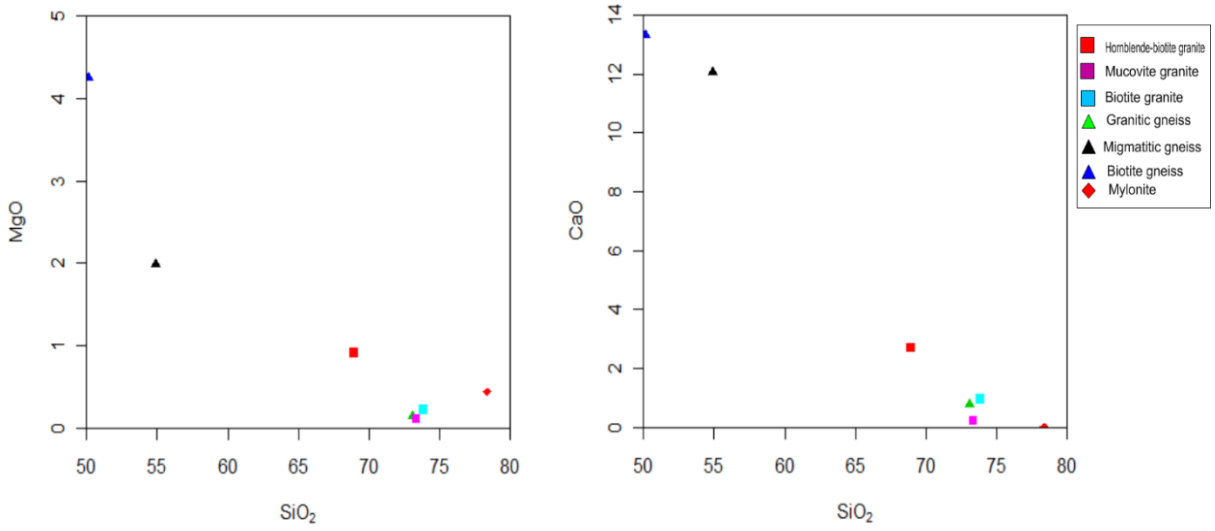

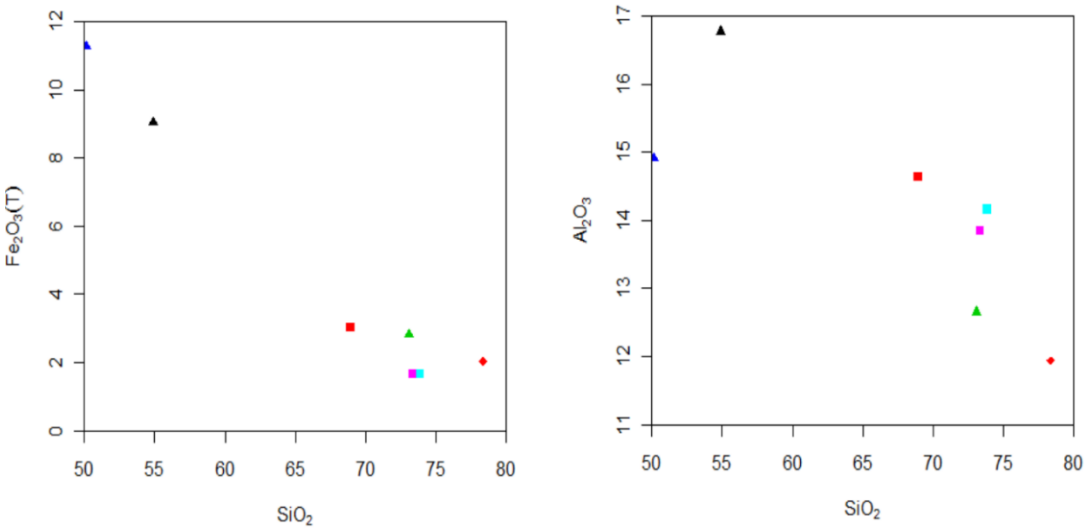

Figure 3a: Harker plots of, MgO, CaO, Fe_2O_3t and Al_2O_3 against silica (SiO_2) for the major rocks in the study area

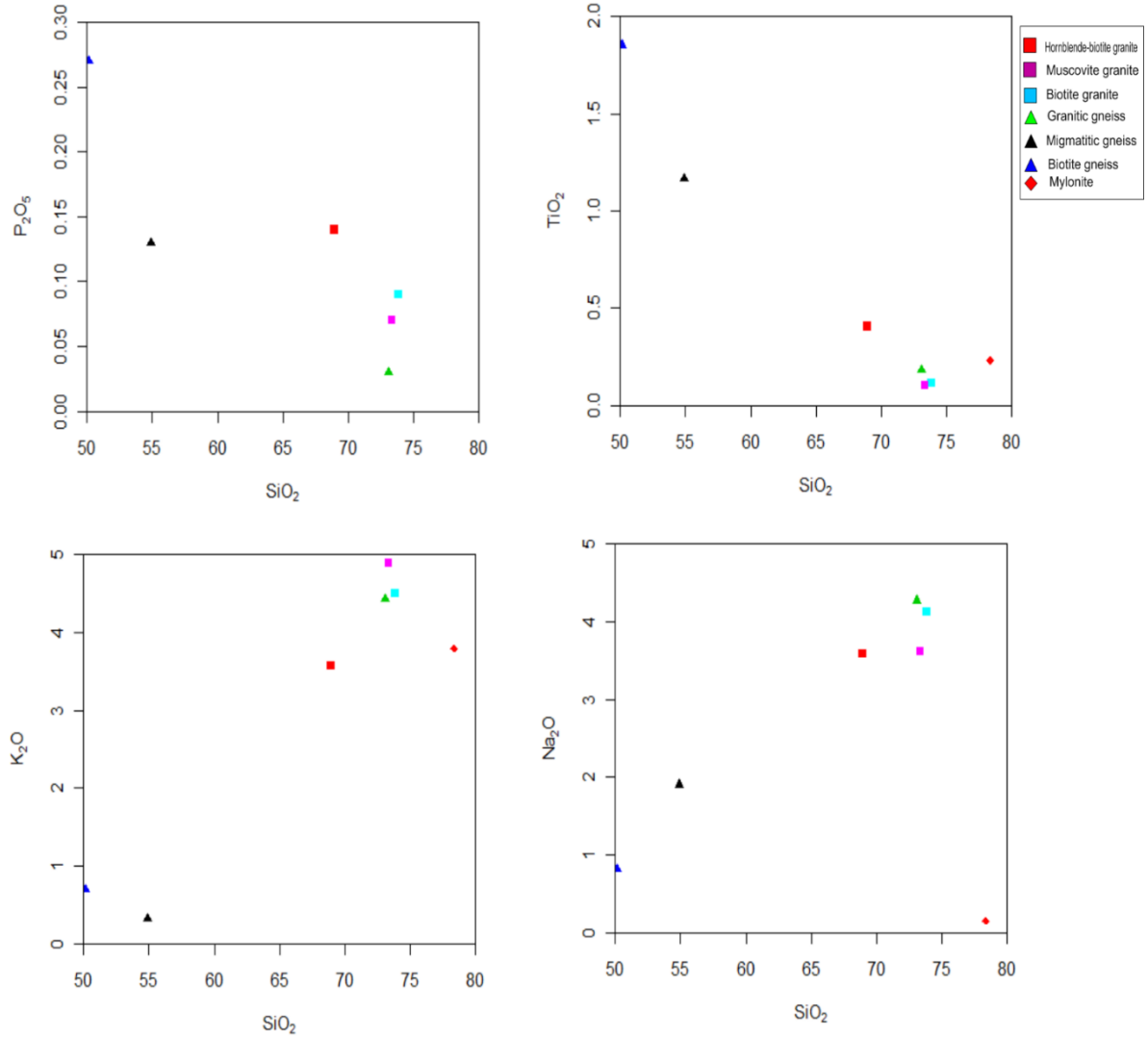

Figure 3b: Harker plots of P_2O_5, TiO_2, K_2O and Na_2O against silica (SiO_2) for the major rocks in the study area

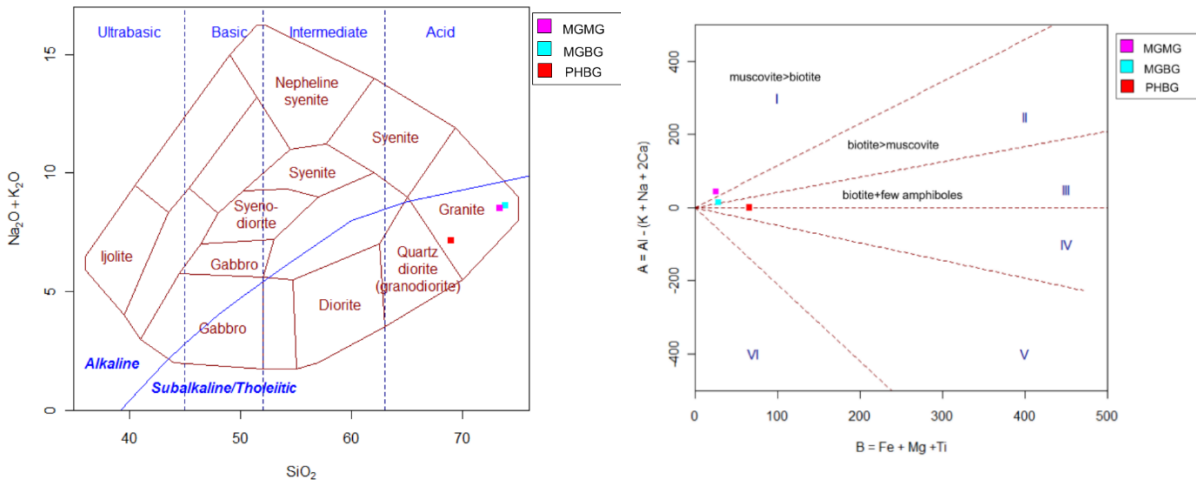

Figure 4: a) Chemical classification of the granites in the study area adapting total alkalis versus silica (TAS) of Cox *et al*., (1979). b) Mineralogical classification of the granites adapting A-B diagram of Debon and Le Forte (1983). (MGMG= medium grained muscovite granite, MGBG=medium grains biotite granite, PHBG=porphyritic hornblende-biotite granite)

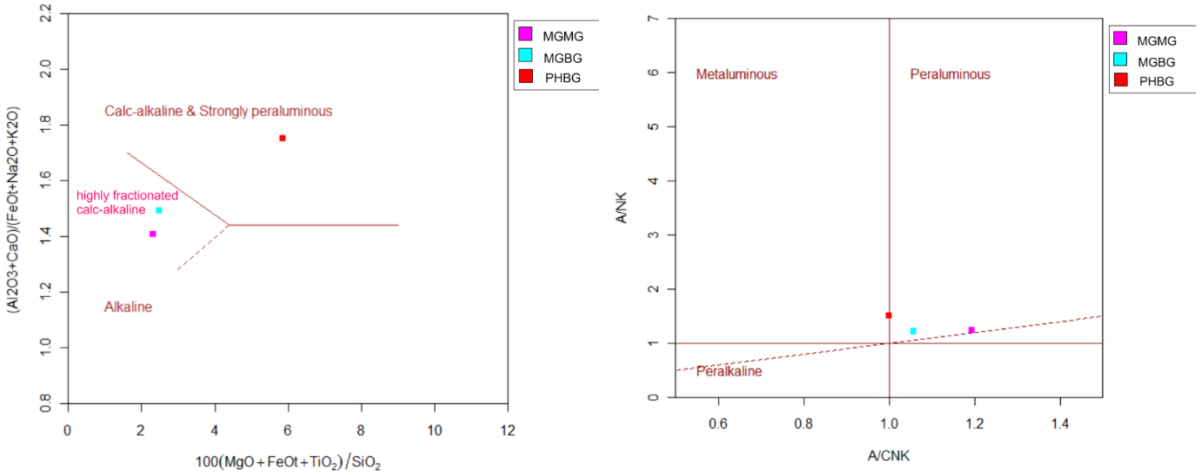

Figure 5: a) Discrimination diagram of the granites after Sylvester (1989). b) A/NK versus A/CNK plots showing the distribution of the granites (after Shand, 1943). (A/NK=Al_2O_3/ (Na_2O + K_2O) A/CNK=Al_2O_3/ (CaO + Na_2O + K_2O)). (MGMG= medium grained muscovite granite, MGBG=medium grains biotite granite, PHBG=porphyritic hornblende-biotite granite)

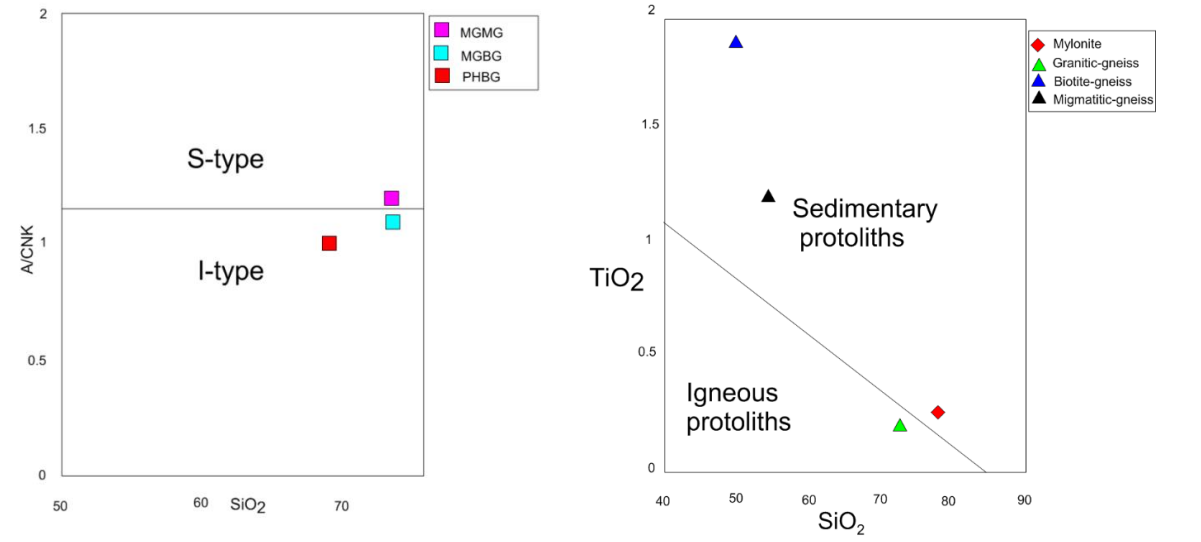

Figure 6: a) Molecular A/CNK (Al_2O_3/CaO+Na_2O+K_2O) versus SiO_2 diagram (after Chappel and White, 1974), showing the classification of the granites. (MGMG= medium grained muscovite granite, MGBG=medium grains biotite granite, PHBG=porphyritic hornblende-biotite granite). b) TiO_2 versus SiO_2 discrimination diagram after (Tarney, 1976) for the gneisses and mylonite in the study area

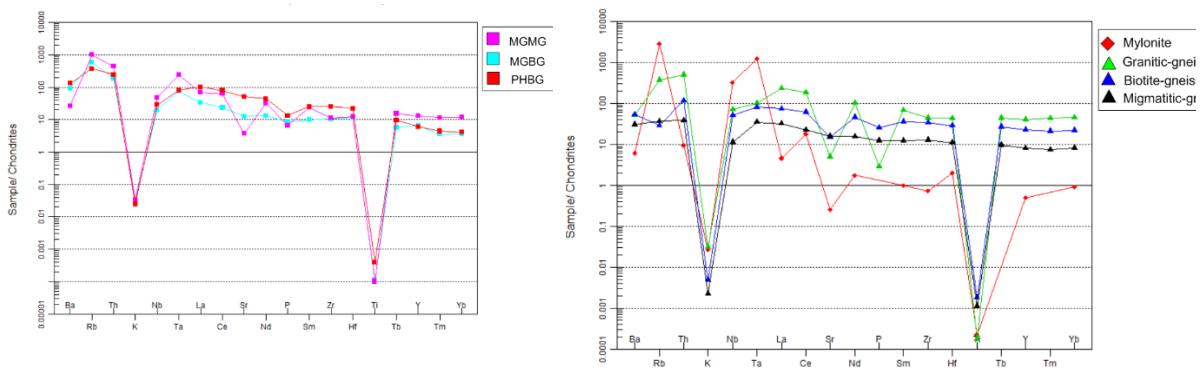

Figure 7: a) Spider plots of trace elements in the granites of the study area. All the plots are normalized to chondrite values after (Thompson 1982). (MGMG= medium grained muscovite granite, MGBG=medium grains biotite granite, PHBG=porphyritic hornblende-biotite granite). b) Spider plots of trace elements in the gneisses of the study area. All the plots are normalized to chondrite values after (Thompson 1982)

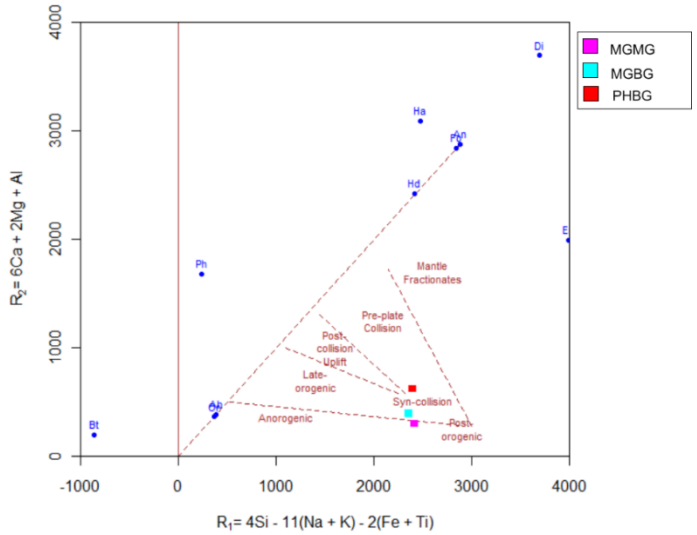

Figure 8: R1-R2 tectonic discrimination diagram after Batchelor and Bowden (1985), with plots of (MGMG= medium grained muscovite granite, MGBG=medium grains biotite granite, PHBG=porphyritic hornblende-biotite granite) in the study area

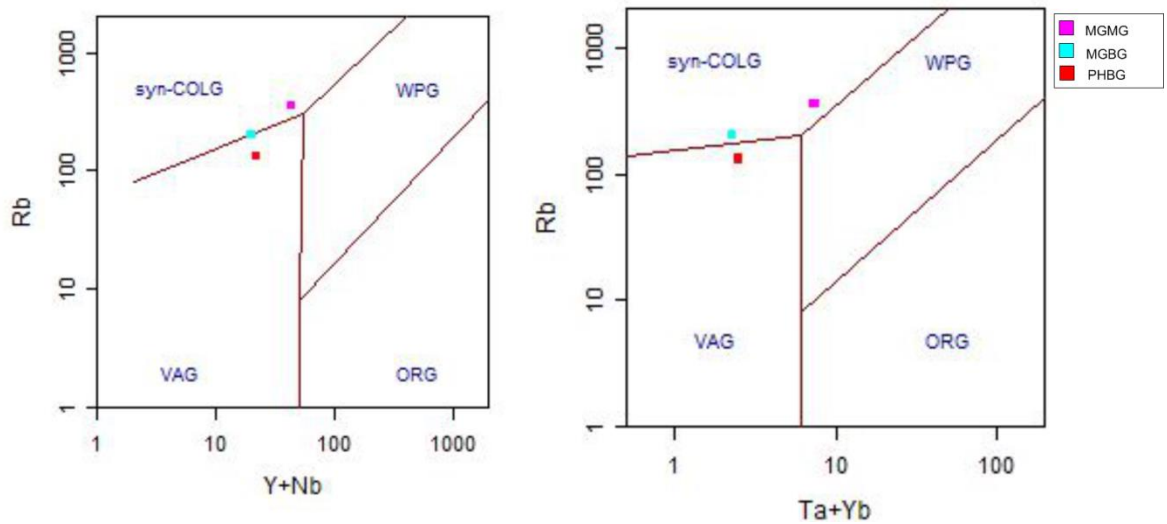

Figure 9: Granite tectonic discrimination diagram (aftet Pearce *et al.*, 1984). (syn-COLG=syn-collisional granites, WPG=within-plates granites, VAG=volcanic-arc granites and ORG=ocean-ridge granites), with plots of (MGMG= medium grained muscovite granite, MGBG=medium grains biotite granite, PHBG=porphyritic hornblende-biotite granite) in the study area

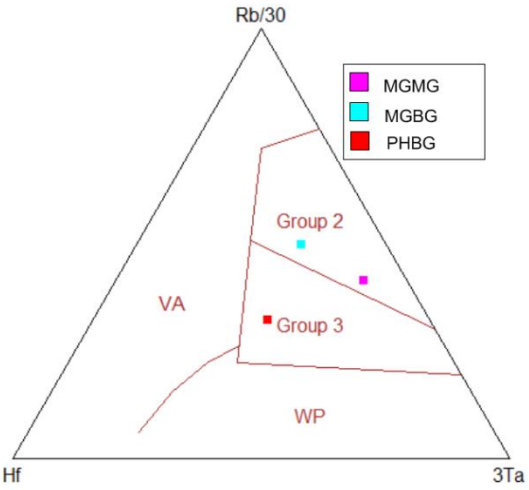

Figure 10: Hf-Rb/10-3*Ta discrimination diagram after Harris *et al*., (1986). (VA=volcanic-arc granites, WP=within-plates granites, Group 2=syn-collisional granites and Group 3=late to post-collisional granites), with plots of (MGMG= medium grained muscovite granite, MGBG=medium grains biotite granite, PHBG=porphyritic hornblende-biotite granite) in the study area.

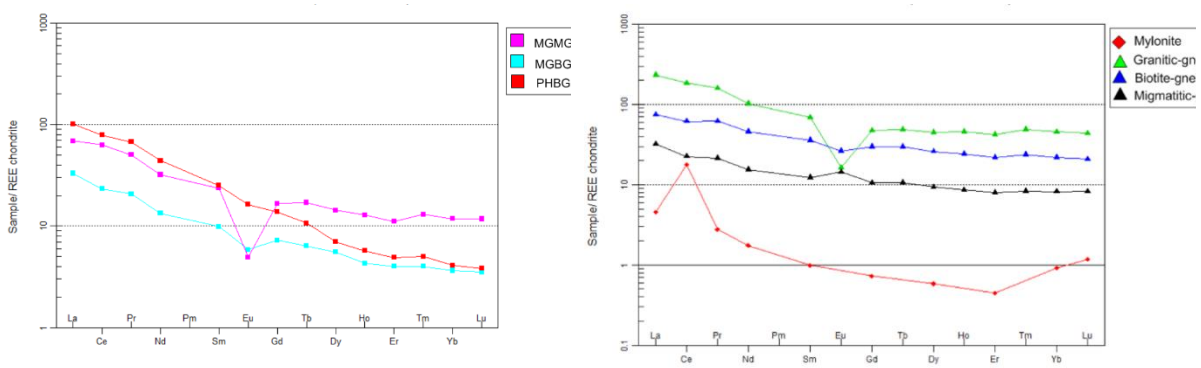

Figure 11: a) Spider plots of REEs in the granites of the study area. All the plots are normalized to chondrite values after (Nakamura, 1974). (MGMG= medium grained muscovite granite, MGBG=medium grains biotite granite, PHBG=porphyritic hornblende-biotite granite). b) Spider plots of REEs in the gneisses of the study area. All the plots are normalized to chondrite values after (Nakamura, 1974)

Discussion

Major elements composition revealed that the gneisses are metaluminous (A/CNK<1) (see table S1 in supplementary data). TiO_2 versus SiO_2 plot (Figure 6b) revealed that migmatite and biotite gneisses are paragneisses (derived from sedimentary protoliths) while granite gneiss is ortho-gneiss (derived from igneous protoliths). The REE pattern of the gneisses (Figure 11b) is somehow straight and parallel except the granite gneiss which has a negative Eu anomaly and this may be due to crystallization of plagioclase during the crystallization of the source rock since it is derived from granite protoliths. Mylonite is granitic in composition, calc-alkaline, strongly peraluminous (A/CNK>1.2), and derived from the metamorphism of sedimentary protoliths as shown in (Figure 6b). Its REE pattern (Figure 11b) shows a positive Ce anomaly indicative of reducing condition.

The B-A plot (Figure 4b) which utilizes some of the major element composition of the granites, classifies the granites into three phases; the muscovite granite plots within the muscovite>biotite field, biotite granite plots within the biotite>muscovite field and hornblende-biotite granite plots within the (biotite + few amphibole) field. This classification is also supported by petrographic studies of the rocks by (Hayatu and Ibrahim 2024). The muscovite and biotite granites are syn-collisional while hornblende biotite granite plots within the volcanic arc-granite field as shown in (Figure 9). According to Pearce (1996), granite suites that straddle the volcanic-arc and within plate fields are products of post-collision setting. This statement is confirmed by (Figure 10) where the porphyritic hornblende biotite granite plots within the Group 3 field (Post-collisional setting). All the granites are calc-alkaline and peraluminous (A/CNK>1) (Figure 5a and b). The peraluminosity increases with increasing differentiation from hornblende biotite granite (1.0) to muscovite granite (1.19). There is similarly enrichment in Rb, Cs, Sn and Nb with depletion in Ba and Sr in the course of evolution from hornblende-biotite granite to muscovite granite. The major element composition of the granites plotted on Harker diagram using SiO_2 as an index of differentiation (Figs. 3a and b) show that TiO_2, Al_2O_3, Fe_2O_3t, MgO, CaO and P_2O_5 are all negatively correlated with SiO_2, forming a well-defined linear trend. Such linear trends might be the result of either hybridization or fractionation (Hassanen *et al.,* 1996) caused by the removal of early formed minerals from the melt. This negative correlation further suggests that the granite suites most likely resulted from fractional crystallization during magmatic evolution. K is strongly depleted in all the granites, while Ba and Sr, which are strongly compatible in granite systems show slight depletion. Sr decreases readily during the course of fractional

crystallization since it replaces Ca in plagioclase while Ba replaces K in K-feldspars as well as in micas, and hence it decreases during the course of fractional crystallization (El Bouseily and El Sokkary 1975). Similarly, according to (Janousek *et al.,* 2002) decrease in Ba with decrease in SiO_2 also indicate an important role of fractionation dominated by biotite, while the depletion of CaO and Sr with increasing SiO_2 content, and negative Eu anomaly is consistent with plagioclase fractionation (Eleftheriadis and Koroneos, 2003). Therefore, variation of these lithophile elements in the granites suggests that fractional crystallization was probably responsible for their evolution. Therefore, the relatively minor negative Eu anomaly especially in hornblende-biotite granite (Figure 11a) that seems to be inconsistent with plagioclase fractionation is probably due to the hornblende fractionation, which minimize the Eu anomaly (Henderson 1984; Eleftheriadis and Koroneos, 2003). Furthermore the negative Ti anomaly observed in the trace element spider diagram (Fig. 7a) suggest the presence of hornblende or Fe-Ti oxides in the source material (Eleftheriadis and Koroneos, 2003).

The granites are depleted in REE (50.71-152.43) compared to the average of 250 ppm (Emmermann *et al.,* 1975). The REE pattern of the granites (Figure 11a) shows enrichment of LREE and depletion of HREE with a weak negative Eu anomaly thus suggesting the fractional crystallization of plagioclase. The less extreme depletion of the HREE relative to LREE may likely be due to low degree of partial melting and presence of amphibole rather than the presence of garnet (because garnet causes extreme depletion of HREE). Moreover, according to (O'Nions and Pankhurst, 1974) enrichment in LREE is the hallmark of crustal and calc-alkaline rocks in general. A/CNK versus SiO_2 plot (Figure 6a) reveals that the hornblende-biotite granite and biotite granite are I-type granites (derived from magmas generated by partial melting of mafic and intermediate igneous rocks) while muscovite granite is S-type granite (derived from magmas generated by partial melting of sedimentary source rock). This can also be seen from CIWP norm result (see table S2 in supplementary data) which show hornblende-biotite granite and biotite granite have low average normative corundum (<1%), high Na_2O (>3.2%) and presence of hornblende which according to Chappel and White (1974), these features are hallmark of I-type granites, while the muscovite granite has average corundum of 2.4 (>1%) which is characteristics of S-type granites. Furthermore, the CIWP norm result has also shown that normative diopside is absent in all the granitites and molecular A/CNK>1 thus suggesting that the granites are S-type.

Petrogenesis of the Rocks

Calc- alkaline rocks are related to subduction related plate tectonic processes. The similarity in patterns of peaks and troughs in the trace element spider plots of gneisses and granites suggests that they share a common parent. Geochemical studies have shown that the gneisses are both ortho-and paragneisses derived from both igneous and sedimentary protolith. I-type granites are likely derived from magmas generated by partial melting of mafic and intermediate igneous rocks, while the S-type granites are likely derived by the partial melting of metamorphosed shales that contain aluminous mica and Al_2O_5 polymorphs thus leading to the generation of peraluminous magma. S-type granites contain aluminous rich minerals in addition to biotite, two feldspars and quartz. Therefore, from the above characteristics, it can be suggested that the granites have a mixed origin and are therefore both I and S-type granites.

CONCLUSION

Based on the geochemical data of the rocks, the geochemical characteristics of the granites are comparable with typical I-type and S-type granites that were emplaced in a syn to post tectonic collisional setting. Thus, the granites can be said to have undergone changes from a more primitive hornblende-biotite I-type variety to a more fractionated muscovite bearing S-type variety. Their source is believed to be from the partial melting of mafic/intermediate igneous rocks and partial melting of metamorphosed shale respectively.

ACKNOWLEDGEMENT

Contributions from Dr. Tavershima Najime of the Department of Geology, Ahmadu Bello University Zaria is hereby acknowledged for his assistance and guidance thorough out this work.

REFERENCES

Ajibade, A. C. (1976). Provisional classification of the Schists Belts of North Western Nigeria In: in Kogbe, C.A Geology of Nigeria, Elizabethan Publishing Company, Lagos, Nigeria:pp85-90.

Ajibade. A. C., Woakes, M., and Rahaman, M. A. (1987). Proterozoic Crustal Development in the Pan-African Regime of Nigeria. In: C. A. Kogbe (ed), Geology of Nigeria 2nd revised edition, Rock View Nigeria limited, Jos: pp. 57-69.

Black, R., Caby, R., Monssine Pouchkin, A., Bayer, R., Bertrand, J. M., Bourllier, A. M., Fabri, J. and Lesquer, A. (1979). Evidence for Late Precambrian plate tectonics in West Africa. *Nature.* **278**: 233–237.

Batchelor, R. A, Bowden, P. (1985). Petrogenetic interpretation of granitoid rock series using multicationic parameters. *Journal of Chemical Geology* **48**: 43–55.

Burke, K. C and Dewey, J. F. (1972). Orogeny in Africa. In: African Geology, T.F.J. Dessauvagie and A.J. Whiteman (eds.), University of Ibadan Press: pp583-608.

Chappell, B. W. and White, A. J. R. (1974). Two contrasting granite types. *Pacific journal geology*, **8**: 173-174.

Chappell, B. W., White. A. J. R. (2001). Two Contrasting Granite Types: 25 years later. *Australian Journal of Earth Sciences* **48:** 489-499.

Cox, K. G., Ball, J. D., Pankhurst, R. J. (1979). The Interpretation of Igneous Rocks. Allen and Unwin, London: p. 450.

Dada, S. S. (1999). Geochemistry and petrogenensis of the reworked gneiss complex of North Central Nigeria: Major and trace elements studies on Kaduna amphibolites and migmatite gneisses. *Global Journal of Pure and Applied Sciences.* **5** (4): 535-543.

Debon, F. and Le Forte, P. (1983). A chemical-mineralogical Classification of common Plutonic Rocks and Association. *Earth Sciences*, **73:** 135-149.

El-Bouseily, A. M. and El-Sokkary A. A. (1975). The relationship between Rb,Sr and Ba in granite rocks. *Journal Of chemical geology* **16:** 207-219.

Eleftheriadis, G., and Koroneos A. (2003). Geochemistry and petrogenesis of post-collision Pangeon Granitoids in Central Macedonia, northern Greece. Chemie der Erde **63** (2)**:** 364–389.

Emmermann, R., Daieva, L., and Schneider, J. (1975). Petrological significance of rare earth distribution in granites. *Contribution to mineralogy and petrology*, **52:** 267-283.

Fitches, W. R., Ajibade, A. C., Egbuniwe, I. G., Holt, R. W., and Wright J. B. (1985). Late Proterozoic Schist belts and plutonism in NM Nigeria. *Journal of Geological Society of London.* **142**: 319–337.

Harker, A. (1909). The natural history of Igneous Rocks. Methuen, London. Pp. 384.

Harris, N. B. W., Pearce, J. A. and Tindle, A. G. (1986). Geochemical characteristics of Collision Zone Magmatism. In: Coward, M.P., Ries, A.C (eds.), Collision Tectonics, Geological Society, London Special Publication, **19:** pp. 67-81.

Hassanen M. A., El-nisr S. A., and Mohamed F. H. (1996). Geochemistry and Petrogenesis of Pan-African I-type granitoids at Gabal Igla Ahmar, Eastern Desert, Egypt. *Journal of African Earth Science* **22** (1)**:** 29-42.

Hayatu and Ibrahim (2024): Field Geology And Petrography Of Basement Rocks Around Makarfi Area, Northwestern Nigeria Basement Complex, Article In press.

Henderson P. (1984): Rare Earth Element geochemistry. Elsevier, Amsterdam: pp. 234- 510.

Janousek V., Vrana S. and Ervan, V. (2002). Petrology, geochemical character and Petrogenesis of a Variscan post-orogenic granite: case study from the Sevetin Massif, Moldanubian batholith, southern Bohemia. *Journal of the Czech Geological Society* **47:** 1-2.

Ogunyele, A., & Akingboye, A. (2018). Tin Mineralisation in Nigeria: A Review. *Environmental and Earth Sciences Research Journal*, *5*(1), 15–23. https://doi.org/10.18280/eesrj.050103.

McCurry, P. (1976). The geology of the Precambrian to Lower Palaeozoic rocks of Northern Nigeria. A review In: C.A. Kogbe, (Editor), Geology of Nigeria. Elizabethan Publication Company, Lagos Nigeria: pp15-39.

Nakamura, N. (1974): Determination of REE, Ba, Fe, Mg, Na and K in Carbonaceous and ordinary Chondrites. *Geochemistry Acta*, **38**: 757-775.

O"Nions, R. K., Pankhurst, R. J. (1974). Rare-earth element distribution in Archean Gneisses and Anorthosites, Godthad area, West Greenland.*Journal Planetary Earth. Science* **22**: 328-338.

Pearce J. A. (1996). Sources and Setting of Granite Rocks. *Episodes*, **19** (4)**:** 120-125.

Pearce J. A., Harris N. B. and Tindle A. G. (1984). Trace element discrimination diagrams for the tectonic interpretation of granite rocks *Journal of Petrology*, **25:** 956 – 983.

Rahaman, M. A. (1976). Review of the Basement Geology of Southwestern Nigeria, in Kogbe, C.A Geology of Nigeria, Elizabethan Publishing Company, Lagos, Nigeria: pp. 41-58.

Rahaman M. A. (1988). Recent Advances in the Study of the Basement Complex of Nigeria in: Geological Survey of Nigeria (ed.) Precambrian Geology of Nigeria: pp11-41.

Shand S. J. (1943). Eruptive Rocks. Their genesis, composition, and classification. John Wiley and sons: pp. 52-103.

Streckeisen, A. L. (1976). To each plutonic rock its proper name. *Earth Science Review* **12**: 1-33.

Sylvester, P. J. (1989). Post Collisional Alkaline Granites. *Journal of Geology*, **97**: 261-280.

Tarney, J. (1976). Geochemistry of Archaean high-grade gneisses with implications as to the origin and evolution of the Precambrian crust. In: Windley, B.F. (Ed.), The Early History of the Earth. Wiley, New York: pp. 405–418.

Thompson, R. N. (1982). British Tertiary Volcanic Province. *Scottish Journal Geolology* **18**: 49-107.

APPENDIX

Table 4: Calculated values of iron number, modified alkali-lime index and aluminium saturation index for the rocks of the study area

Sample	Iron number (Fe no)	Modified alkali-lime index (MALI)	Aluminum saturation index (ASI)
R1	0.81	3.93	2.75
R2	0.95	7.94	0.96
R3	0.70	-11.82	0.57
R4	0.87	7.68	1.07
R5	0.93	8.30	1.20
R6	0.75	4.48	1.01
R7	0.80	-9.84	0.66

Legend; R2= Granitic gneiss. R4=Medium grained biotite granite R3=Biotite gneiss R5=Medium grained muscovite granite R7=Migmatitic gneiss R6=Porphyritic hornblende-biotite granite R1= Mylonite

Table 5: CIWP Norm for the granites of the study area

Normative minerals	Medium grained biotite granite	Medium grained muscovite granite	Porphyritic hornblende-biotite granite
Q	30.495	33.222	27.680
C	0.983	2.422	0.322
Or	26.594	28.998	21.098
Ab	34.947	30.547	30.378
An	4.125	0.535	12.381
Di	0	0	0
Wo	0	0	0
Hy	0.548	0.274	2.267
Ti	0.051	0.079	0.103
Tn	0	0	0
Ru	0.086	0.061	0.351
Ap	0.213	0.166	0.332
Sum	98.042	96.204	94.911